J Solid State Electrochem (2008) 12:1061–1066
DOI 10.1007/s10008-007-0427-9

ORIGINAL PAPER

Reversible lithium intercalation in disordered carbon prepared from 3,4,9,10-perylenetetracarboxylic dianhydride

Zonghui Yi · Xiaoyan Han · Changchun Ai · Yongguang Liang · Jutang Sun

Received: 1 June 2007 / Revised: 30 August 2007 / Accepted: 2 September 2007 / Published online: 27 September 2007

Abstract The electrochemical properties of the 3,4,9,10-perylenetetracarboxylic dianhydride (PTCDA)-based carbon, synthesized by directly pyrolyzing PTCDA under an argon gas flow, have been firstly explored as an anode material for lithium-ion batteries. PTCDA is decomposed in a single-step reaction, which was completed around 650 °C. X-ray diffraction studies indicated a disordered carbon structure, and scanning electron microscopy (SEM) results revealed that this PTCDA-based carbon had a pillar-like morphology with a diameter of approximately 1–4 μm and length of 5–20 μm. Electrochemical measurements showed that it delivered lithium insertion and deinsertion capacities of 496 and 311 mAh g^{-1}, respectively, during the first cycle. The charge capacity retention from the 1st to the 50th is 93.2% with an average capacity fade of 0.14% per cycle. The coulombic efficiency of the Li insertion/deinsertion processes reached 99% after five cycles.

Keywords 3,4,9,10-Perylenetetracarboxylic dianhydride · PTCDA-based carbon · Disordered carbon · Anode materials · Lithium-ion batteries

Introduction

Lithium-ion batteries have long been an attractive power source for a wide variety of applications. Carbon materials are the major one for the negative electrode in the rechargeable lithium battery. Different types of carbon materials, such as graphitic carbon, carbon nanotubes, and disordered carbon, have been intensively investigated as anode materials for lithium-ion batteries, and several models have been proposed to explain lithium-ion intercalation and storage in these carbon materials [1–10].

Graphite is widely used as the anode in commercial cells due to its very flat potential and structural stability upon cycling, but its disadvantages are high cost and low specific capacity (normally below 372 mAh g^{-1} under ambient conditions) [11–13]. Recently, carbon nanotubes with a large surface area have drawn interest from the battery industry. However, a high irreversible capacity (460–1080 mAh g^{-1}), together with a relatively low reversible capacity (100–400 mAh g^{-1}), has been observed [8, 14, 15]. The use of disordered carbon makes it possible to satisfy the increasing worldwide demand for high energy density batteries nowadays. Disordered carbon, despite its large irreversible capacity and hysteresis, has many appealing features like [2, 6, 10, 16–21] (1) high specific capacity, (2) their amenability to doctoring by varying the organic precursors and temperature, and (3) good cycling ability. Therefore, the study and optimization of disordered carbon remains an important point in developing new high-performance batteries.

Among the disordered carbonaceous substance studied, one obtained from the pyrolysis of such condensed aromatics as poly-paraphenylene, pitch, and poly-acenic materials was reported to have a specific capacity of up to 700 mAh g^{-1} [2, 22–26].

3,4,9,10-Perylenetetracarboxylic dianhydride (PTCDA, Scheme 1) belongs to a kind of unique condensed aromatics with a highly developed conjugated π-electronic structure. Recently, PTCDA and its derivative compounds have aroused much interest among researchers. They represent one of the most widely studied classes of organic semi-

Z. Yi · X. Han · C. Ai · Y. Liang · J. Sun (✉)
Department of Chemistry, Wuhan University,
Wuhan 430072, People's Republic of China
e-mail: jtsun@whu.edu.cn

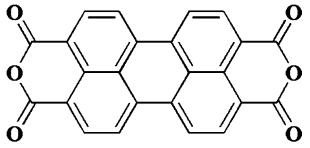

Scheme 1 Schematic of 3,4,9,10-perylenetetracarboxylic dianhydride

conductors with possible use for various photonic and electronic applications [27–30].

PTCDA is expected to be a wonderful precursor for pyrolytic carbon as a negative electrode for lithium-ion batteries due to its unique structure, appealing property (e.g., molecular self-assembly) [31–33], high melting point, and high pyrolytic yield.

In this work, a new kind of disordered carbon with a pillar-like morphology prepared by low-temperature (700 °C) pyrolysis of PTCDA is investigated for the first time as an anode material for lithium ion batteries. It is found that this PTCDA-based carbon exhibits unusual electrochemical characteristics.

Experiment

Material preparation and characterization

PTCDA was pyrolyzed without further purification under an argon atmosphere at a rate of 25 °C/min from room temperature to 700 °C where the substance was heat-treated for another 1h.

Thermogravimetry analysis (TG) of PTCDA was performed by the Setaram Setsys 16 TG-DTA/DSC Instrument (France) at a heating rate of 10 °C/min in argon. The elemental analysis (EA) of the PTCDA-based carbon was carried out using VarioEL III (Germany). The Fourier transform infrared (FTIR) spectrum (Thermo Nicolet Avatar 360) was used to identify the functional groups present before and after the thermal treatment. The X-ray diffraction (XRD) measurement was carried out with a Shimadzu XRD6000 diffractometer with Cu-Kα_1 radiation (λ = 1.54056 Å). Data was collected between 10 and 80° with a scan speed of 4°/min. The particle size and morphological features were revealed by a scanning electron microscope (Hitachi SEM 400).

Electrochemical measurement

Electrochemical experiments were carried out in a coin-type cell (size, 2,016), using PTCDA-based carbon as a working electrode and lithium foil as a counter electrode. Electrode was prepared by mixing PTCDA-based carbon powders with 15 wt% acetylene black and 5 wt% polytetrafluoroethylene binder, compressing the mixture onto a nickel gauze current collector. The electrolyte was the solution of 1 mol l^{-1} $LiPF_6$ dissolved in a 1:1 mixture of ethylene carbonate (EC) and dimethyl carbonate (DMC) by volume. A porous polypropylene film (Celgard 2300) was used to separate two electrodes. The cell was assembled in an argon-filled glove box. The cell was discharged and charged between 3.0 and 0.001 V vs metallic lithium at a constant current density of 100 mA g^{-1}. Electrochemical measurement of the cell was performed at room temperature.

Result and discussion

The TG curve of the PTCDA precursor is shown in Fig. 1. From the TG curve, the pyrolysis of the precursor proceeds from 490 to 650 °C. The corresponding mass loss is mainly caused by two factors: one is probably due to the release of CO and CO_2, resulting from the thermal decomposition of

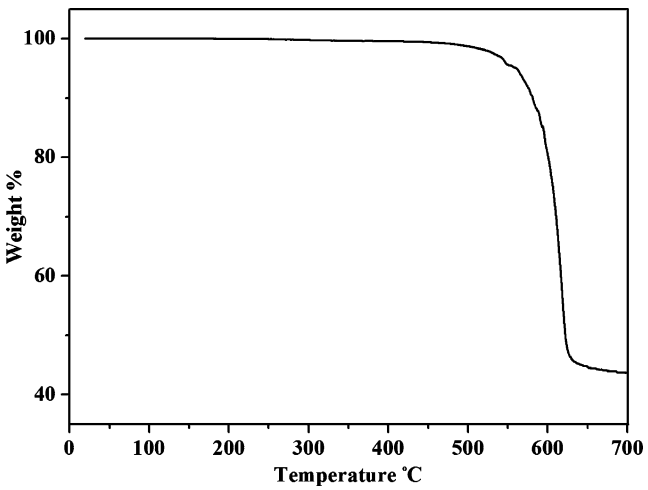

Fig. 1 TG curve of the PTCDA precursor

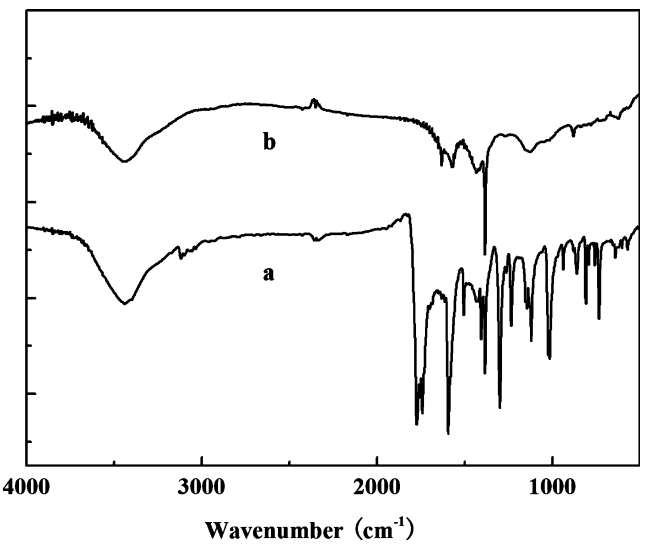

Fig. 2 IR spectra for **a** PTCDA and **b** PTCDA-based carbon

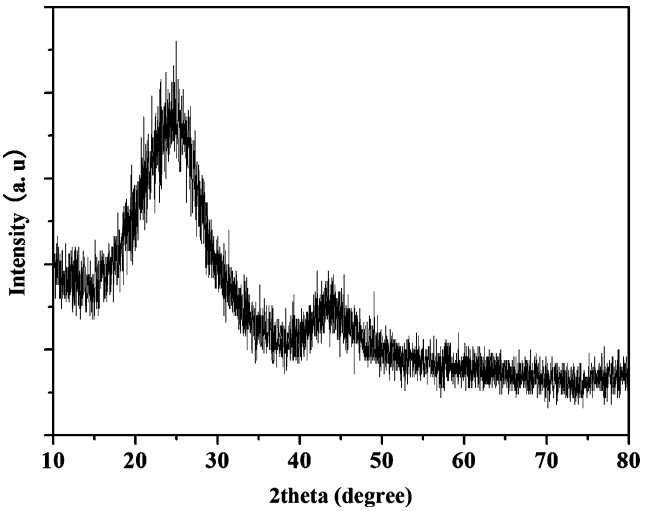

Fig. 3 XRD pattern of PTCDA-based carbon

dianhydride substituents; the other is associated with the loss of H_2 and low-volatile organics, resulting from the gradual thermal degradation of the aromatic structure. The degradation curve illustrates that the carbon structure begins to form at a temperature above 600 °C, and the mass of the product at 700 °C is about 44% of that of the PTCDA precursor.

The results of elemental analysis are C, 90.4, H, 0.9, O, 8.7 (wt%), with an approximate composition $H_{0.12}CO_{0.07}$. Despite the presence of adsorbed water, which results from exposing the pyrolytic carbon to air, that is confirmed by the IR spectrums in Fig. 2b, this PTCDA-based carbon is expected to exhibit a good electrochemical behavior due to the almost thorough removal of elemental O during thermal treatment process. It was reported that substantial amount of elemental O might be detrimental to the electrochemical property of carbon materials. It was found that elemental O was associated with high irreversible capacity of carbon electrode [34].

The FTIR spectra of PTCDA and PTCDA-based carbon are shown in Fig. 2. The spectrum of PTCDA (Fig. 2a) consists of absorptions at 1,775 cm^{-1} (C=O vibration); 1,741 cm^{-1} (aromatic $^{\delta}C-H$, out of plane); 1,596, 1,505, 1,405, and 1,380 cm^{-1} (aromatic C=C vibration); 1,299, 1,232 cm^{-1} (C–O–C); and 858, 812,

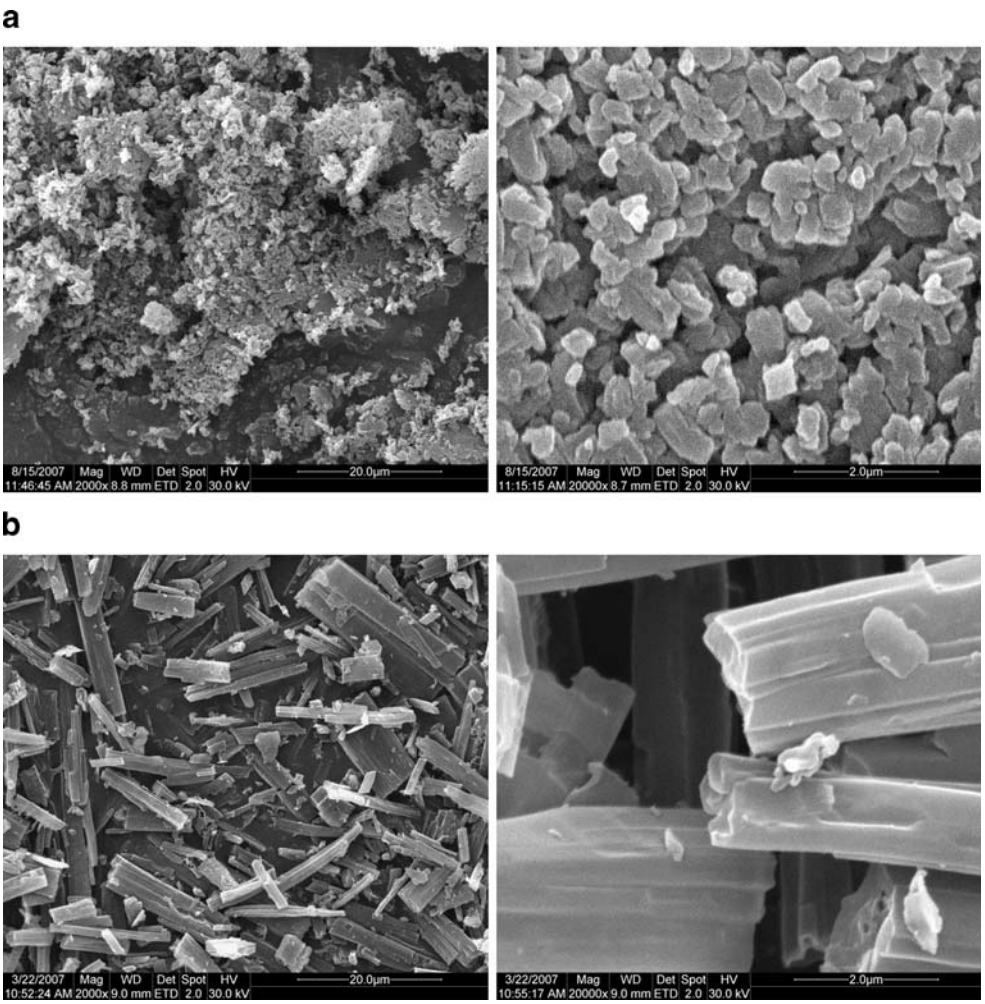

Fig. 4 SEM images of precursor PTCDA (**a**) and as-prepared PTCDA-based carbon (**b**)

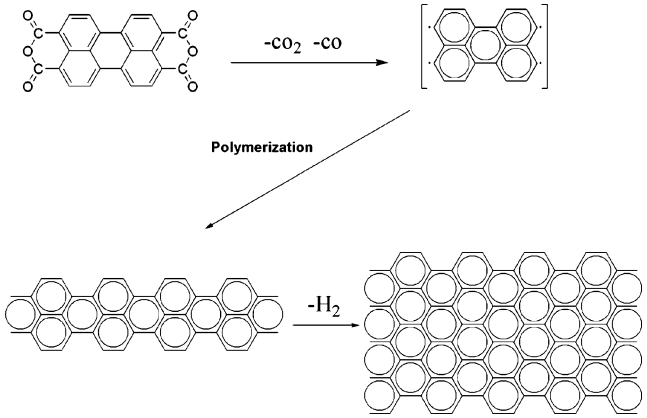

Scheme 2 Schematic of the possible polymerization mechanism of PTCDA molecule

and 734 cm^{-1} (aromatic $^{\delta}C-H$, out of plane). The organic functional groups are dramatically removed at 700 °C (shown in Fig. 2b). Absorptions based on dianhydride substituents completely disappear. The absorption bands for aromatic C=C vibration and aromatic $^{\delta}C-H$ become broadened as in the case of conventional carbons.

The XRD patterns of the PTCDA-based carbon are presented in Fig. 3. The XRD patterns are indicative of a disordered carbon system. The broad (002) reflection peak, located at about 2θ = 25°, indicates that the sample is composed of some small domains of graphene sheets with a low graphitization degree. The (002) peak position measures the average spacing between adjacent graphene sheets in the carbon. The interlayer spacing is calculated using the Bragg equation.

$$d_{002} = \lambda/(2\sin\theta)$$

According to the above equation, the d_{002} of PTCDA-based carbon is about 0.356 nm, which is a little larger than that of pure graphite carbon (about 0.335 nm). A larger interlayer spacing is thought to be favorable to retaining the structure stability of electrode during lithium insertion and extraction process. In addition, the broad (100) peak is clearly observed at 2θ near 43.7°, indicating that this PTCDA-based carbon is definitely made up of small graphene sheets [22].

The SEM photographs of PTCDA and PTCDA-based carbon are shown in Fig. 4. Figure 4a shows images of PTCDA crystals before pyrolysis. Figure 4b reveals that PTCDA-based carbon is mainly composed of pillar-shaped carbon with a diameter of approximately 1–4 μm and length of 5–20 μm. It is obvious that the shape of PTCDA-based carbon is quite different from that of PTCDA precursor. There is no direct correlation between their shape before and after pyrolysis. As PTCDA is a molecular crystal and no strong chemical bonds exist between the molecules, the rearrangement of the formed molecular fragments in the process of thermal decomposition could occur very easily. The surface of this carbon (including the edge surface) is found to be smooth. The smoothness of the surface may favor reduction of the number of active sites on the carbon surface and therefore decrease of the irreversible capacity loss during the lithiation process [35]. Some carbon flakes can also be seen attached to big pillar-like carbon. It is very possible that the PTCDA molecule started to decarboxylize and form perylene-tetraradicals, when PTCDA was heated to a certain temperature. The adjacent perylene-tetraradicals polymerized together immediately. Then, some monolayer carbon sheet formed by further dehydrogenation of aromatic oligomers at a higher temperature. The pillar-shaped carbon materials were obtained by the gradual stack of monolayer carbon sheets approximately parallel to each other until the PTCDA molecules were exhausted [36]. The whole process can be formulated as shown in Scheme 2. Compared to common

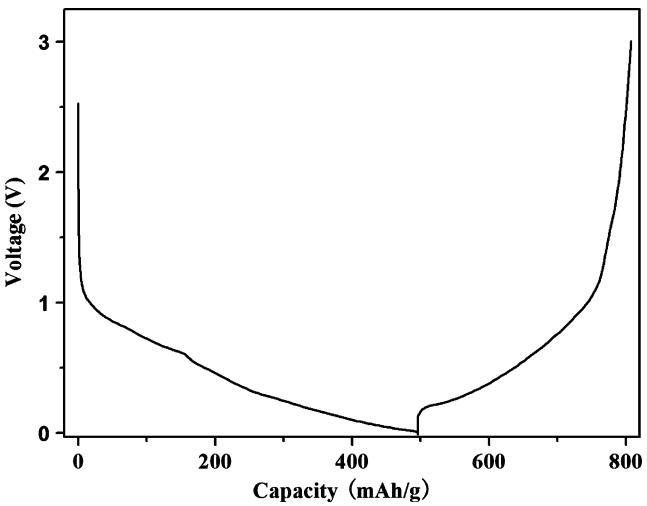

Fig. 5 The first discharge–charge curve of PTCDA-based carbon electrode at a current density of 100 mA g^{-1} between 3.0 and 0.001 V

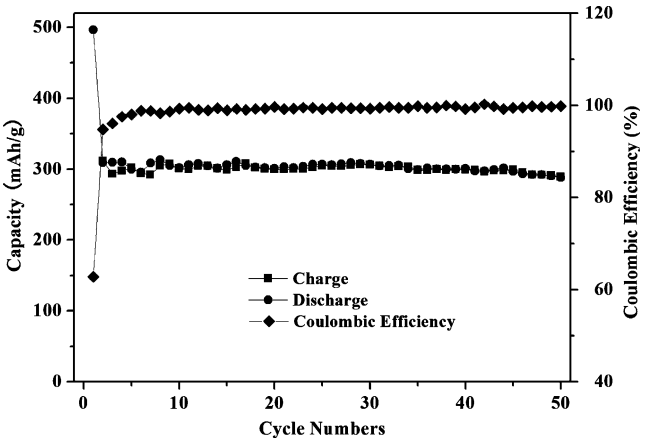

Fig. 6 Cycle performance of PTCDA-based carbon at a current density of 100 mA g^{-1} between 3.0 and 0.001 V

pyrolytic carbon, this PTCDA-based carbon has a relatively regular morphology, less surface area, and lower surface activity, suggesting a better electrochemical performance during cycling.

Many parameters of carbon, such as chemical composition, crystallite size, interlayer spacing, surface morphology, and surface area, affect the electrochemical property. Figure 5 shows the typical discharge and charge curves of PTCDA-based carbon/Li test cell at a moderate current density of 100 mA g^{-1} in the first cycle. The potential profile differs radically from that of graphite: no stages or Li intercalation via phase transition at a narrow potential range, but rather a sloping lithium insertion voltage between 0 and 1.5 V, indicating a model for lithium-ion insertion into this PTCDA-based carbon different from that for lithium–graphite intercalation compounds (Li-GIC). Generally, carbons prepared by low-temperature (500–1,000 °C) pyrolysis of organic precursors show a large hysteresis, which is mainly related to lithium doping at the inner surface of the cavities constructed by the edges of disordered staking of crystallites [37]. However, no obvious hysteresis is observed on the voltage profile of PTCDA-based carbon. As the highly developed conjugated π-electronic structure of the PTCDA precursor favors the growth of graphene, very few cavities are formed when most of graphene sheets approximately parallel to each other gradually stack to crystallites with orientation to some extent.

The initial discharge capacity is as high as 496 mAh g^{-1} and the loss of capacity is about 185 mAh g^{-1}, mainly caused by the formation of solid–electrolyte interface (SEI) films. Besides SEI films, the reactions of Li with surface functional groups and absorbed molecules (e.g., H_2O and CO_2) and the irreversible insertion of Li on the hydrogen-terminated edges of graphene sheets also contribute to a fraction of irreversible capacity. The reversible capacity in the first process shows about 311 mAh g^{-1}. The initial coulombic efficiency is 62.7%.

Figure 6 shows the cycling characteristics of the electrode at a current density of 100 mA g^{-1} within 50 cycles. It is obvious that the electrode displays an outstanding cycling ability. The progressive drop in capacity, which is common in low-temperature pyrolyzed carbons, is not observed in this PTCDA-based carbon electrode, indicating that the surface and microstructure characteristics of PTCDA-based carbon favor to form effective and stable SEI film [5, 10, 38]. The charge capacity of the electrode is still 290 mAh g^{-1} after 50 cycles. The charge capacity retention from the 1st to the 50th is 93.2% with an average capacity fade of 0.14% per cycle. The efficiency of the Li insertion/deinsertion processes gradually increases and reaches 99% after five cycles.

Conclusions

In this work, a new kind of PTCDA-based carbon with a pillar-shaped morphology was obtained by directly pyrolyzing PTCDA at 700 °C under argon atmosphere. XRD studies showed that the PTCDA-based carbon was disordered. Charge–discharge results exhibited a large specific capacity and a satisfied cycling stability. The economical preparation process and excellent electrochemical behavior make this kind of PTCDA-based carbon a great potential as an anode material for lithium ion batteries.

Acknowledgements This work was supported by the National Natural Science Foundation of China (No. 20771087).

References

1. Iijima T, Suzuki K, Matsuda Y (1995) Synth Met 73:9
2. Sato K, Noguchi M, Demachi A, Oki N, Endo M (1994) Science 264:556
3. Inagaki M, Iwashita N, Hishiyama Y (1994) Mol Cryst Liq Cryst 244:89
4. Mabuchi A, Tokumitsu K, Fujimoto H, Kasuh T (1995) J Electrochem Soc 142:1041
5. Zheng T, Liu Y, Fuller EW, Tseng S, Sacken U, Dahn D (1995) J Electrochm Soc 142:2581
6. Takami N, Satch A, Ohsaki T, Kanda M (1997) Electrochim Acta 42:2537
7. Yoshio M, Wang H, Lee YS, Fukuda K (2003) Electrochim Acta 48:791
8. Skowronski JM, Knofczynski K, Yamada Y (2003) Solid State Ionics 157:133
9. Xiang H, Fang S, Jiang Y (1999) Carbon 37:701
10. Zheng T, Xue JS, Dahn JR (1996) Chem Mater 8:389
11. Yazami R (1999) Electrochim Acta 45:87
12. Ohzuku T, Iwakoshi K, Sawai K (1993) J Electrochem Soc 140:2490
13. Megahead S, Scosati B (1994) J Power Sources 51:79
14. Frackowiak E, Grautier S, Graucher H, Bonnamy S, Beguin F (1999) Carbon 37:61
15. Wu G, Wang CS, Zhang XB, Yang HS, Qi Z, He P, Li W (1999) J Electrochem Soc 146:1696
16. Yazami R, Deschamps M (1995) J Power Sources 54:411
17. Zhou H, Zhu S, Hibino M, Honma I, Ichihara M (2003) Adv Mater 15:2107
18. Fey GTK, Chen KL, Chang YC (2002) Mater Chem Phys 76:1
19. Lee KT, Lytle JC, Ergang NS, Oh SM, Stein A (2005) Adv Mater 15:547
20. Matsumura Y, Wang S, Mondori J (1995) Carbon 33:1457
21. Tokumitsu K, Mabuchi A, Fujimoto H, Kasuh T (1996) J Electrochem Soc 143:2235
22. Gong J, Wu H, Yang Q (1999) Carbon 37:1409
23. Yata S, Kinoshita H, Komori M, Ando N, Kashiwamura T, Harada T, Tanaka K, Yamabe T (1994) Synth Met 62:153
24. Sato Y, Kikuchi Y, Nakano T, Okuno G, Kobayakawa K, Kawai T, Yokoyama A (1999) J Power Sources 81–82:182
25. Park CW, Yoon SH, Lee SL, Oh SM (2000) Carbon 38:995
26. Yata S, Hato Y, Kinoshita H, Ando N, Anekawa A, Hashimoto T, Yamguchi M, Tanaka K, Yamabe T (1995) Synth Met 73:273

27. Forrst SR et al (1984) J Appl Phys 55:1492
28. Lee SK, Zu Y, Herrmann A, Geerts Y, Mullen K, Bard AJ (1999) J Am Chem Soc 121:3513
29. Sadari M, Hadel L, Husain RR, Krogh-Jespersen K, Westbrook JD, Bird GR (1992) J Phys Chem 96:7988
30. Debreczeny MP, Svec WA, Marsh EM, Wasielewski MR (1996) J Am Chem Soc 118:8174
31. He P, Lefevre M, Faubert G, Dodelet JP (1999) J new Mater Electrochem Systems 4:243
32. Faubert G, Cote R, Dodelet JP, Lefevre M, Bertrand P (1999) Electrochim Acta 15:2589
33. Kamiya K, Noda T, Ide M, Tanaka J (1995) Synth Met 71:1765
34. Xing W, Dahn JR (1997) J Electrochem Soc 144:1195
35. Aurbach D, Teller H, Levi E (2002) J Electrochem Soc 149:A1257
36. Murakami M, Yoshimura S (1985) Mol Liq Cryst 118:95
37. Xiang HQ, Fang SB, Jiang YY (1999) Carbon 37:709
38. Lee JK, Au KW, Ju JB, Cho BW, Park D, Yun KS (2001) Carbon 39:1299